

Electronic Supporting Information

Swapping Conventional Salts with Entrapped Lithiated Anionic Polymer: Fast Single-Ion Conduction and Electrolyte Feasibility in LiFePO₄/Li Batteries[†]

Soujanya Gowdani,^{1,2,3} Pratyay Basak^{1,2,3,}*

Nanomaterials Laboratory, Inorganic & Physical Chemistry Division,
¹Council of Scientific & Industrial Research-Indian Institute of Chemical Technology (CSIR-IICT);
²CSIR – Network Institutes for Solar Energy (CSIR-NISE) &
³Academy of Scientific and Innovative Research (AcSIR),
Hyderabad-500 007; Andhra Pradesh, INDIA.

Ph(O): 040-27193225/27191386, Fax: +91-40-27160921
Email: pratyay@iict.res.in, pratyaybasak@gmail.com

**To whom all Correspondences should be addressed*

Experimental

Characterizations: The ^1H - and ^{13}C -NMR of the samples dissolved in D_2O as solvent were collected on INNOVA-500 MHz and AVANCE-300 MHz spectrometer at ambient temperature for structural confirmation. The X-ray diffraction (XRD) patterns of the materials were collected on a PANalytical Empyrean XRD equipment in the reflection mode using a zero background sample holder. Incident radiation was generated using a $\text{CuK}\alpha$ source, $\lambda = 1.5406 \text{ \AA}$ and data were collected in the 2θ range, 5° to 70° in continuous scanning mode with a step size of 0.01° using a Pixel 3D detector. X-ray diffraction (XRD) patterns were collected on a PANalytical Empyrean XRD equipment. ESI-MS and MALDI-TOF analysis were carried out on a Waters Micromass and Shimadzu Spectrometers respectively. Fourier transform infrared spectroscopy (FTIR) was used to follow the formation of the hybrid organic-inorganic polymer nanocomposite matrices and the salt solvation in the mid-FTIR absorption range of $4000 - 400 \text{ cm}^{-1}$ employing a Bruker ALPHA-T instrument. Typically, monomer/polymer samples ($\sim 2\text{-}5 \text{ mg}$) were grinded with KBr ($\sim 200 \text{ mg}$) and pressed into transparent pellets of approximate dimensions, $\Phi = 1.2 \text{ cm}$ and $t = 0.02 \text{ cm}$; followed by vacuum drying at 60°C for 30 minutes prior to each run. The transmittance spectra collected for 256 scans with a resolution interval 2 cm^{-1} , were corrected for baseline, atmospheric interference and also normalized when required before comparative evaluation. Morphological studies on the synthesized films were carried out on a Field Emission Scanning Electron Microscope (FESEM), Model: 7610F JEOL. The films were mounted on the stubs both laterally and transversely to study the surface as well as the fractured cross-sections. The thermal stabilities of the functionalized nanomaterials were assessed by a TA Q50 thermogravimetric analyzer. Thermogravimetric scans were recorded at a ramp rate of $10^\circ \text{C}/\text{min}$ under nitrogen atmosphere for 10 to 20 mg samples in the temperature range 35°C to 800°C . Differential scanning calorimetry was performed on a DSC Q200 differential scanning calorimeter (TA Instruments) under dry nitrogen atmosphere. The synthesized organic-inorganic hybrid samples were vacuum dried overnight before carrying out the thermal studies. Typically, a sample of 15-20 mg was loaded in an aluminum pan and hermetically sealed, rapidly cooled down to -150°C using liquid nitrogen, equilibrated for 5 minutes and then heated up to 200°C at a scan rate of $10^\circ \text{C}/\text{min}$. The power and temperature scales were calibrated using pure indium and an empty aluminum pan was used as the reference. Analysis of the thermograms was carried out using universal analysis software provided by the TA Instruments. The glass transition temperature (T_g) was determined from the inflection-point of the transitions. The estimated experimental error in the determination of the glass transition temperature (T_g) is $\pm 2^\circ \text{C}$. Melting and crystallization temperatures, when they occurred, were defined as the maxima of the melting endotherms (T_m) and crystallization exotherms (T_c), respectively.

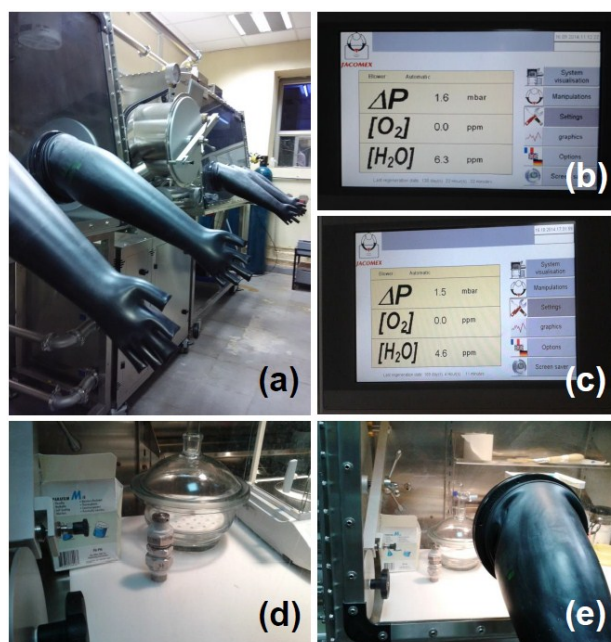


Figure SI-1. (a) A JACOMEX GP[CONCEPT]-T3+T2 glove box unit filled with ultrahigh purity argon (99.999%, IOLAR grade) continuously circulating over a purification bed is used for handling the electrolyte samples; (b) and (c) the operation control unit monitor depicting the status of the unit with respect to oxygen and moisture level over a period of one month; (d) and (e) a typical swagelok-cell assembled inside the glove box unit.

The alternating current (*ac*-) electrochemical impedance spectroscopy (EIS) for the synthesized organic-inorganic hybrid polymer-nanocomposite electrolytes of various compositions were carried out on a Zahner® Zennium electrochemical workstation controlled by Thales Operational Software. The synthesized electrolyte samples were invariably vacuum dried overnight before carrying out the electrical measurements. A JACOMEX make, GP[CONCEPT]-T3+T2 glove box unit filled with ultrahigh purity argon (99.999%, IOLAR grade) continuously circulating over a purification bed was used to handle all samples under inert environment and assemble the cells. The moisture levels and oxygen content in the environment are always maintained at < 10ppm and < 1ppm, respectively. Pelleted circular discs of area $\sim 0.98 \text{ cm}^2$ and thickness $\sim 0.08 \text{ cm}$ were sandwiched between two 316 stainless steel blocking electrodes along with a Teflon spacer of appropriate dimension and loaded in the leak-proof Swagelok assembly. A spring and the Teflon spacer ensured the application of similar pressure and sample geometry during the sample mounting and throughout the test. The sample holders were placed in a controlled heating chamber to carry out the variable temperature impedance measurements over a range of $\sim 20 \text{ }^\circ\text{C}$ to $90 \text{ }^\circ\text{C}$ at an interval of $\sim 5\text{-}7 \text{ }^\circ\text{C}$ during heating. The temperature was measured with accuracy better than $\pm 0.1 \text{ }^\circ\text{C}$ using a K-type thermocouple placed in close proximity with the sample. Samples were equilibrated at each temperature for 30 minutes prior to acquiring the frequency sweep impedance data. All data were collected following a frequency sweep through 1 Hz to 4 MHz range at an alternating potential with a RMS-amplitude of $\pm 10 \text{ mV}$ across the OCV of the assembled cells. No corrections for thermal expansion of the cells were carried out. The real part of the impedance was appropriately normalized for the cell dimensions to determine ionic conductivity (σ (Scm⁻¹

1)). All the data point plotted represents an average of at least three different sets of measurements under similar conditions with appropriate standard deviation provided as Y-Error. Equivalent circuit simulation was done using Zman 2.0 analysis software while the temperature dependence of the ionic conductivity data (Arrhenius, V-T-F), Lorentzian fits and power law fittings were done using non-linear least square fits (NLSF) available in Microcal OriginPro 8.5 software.

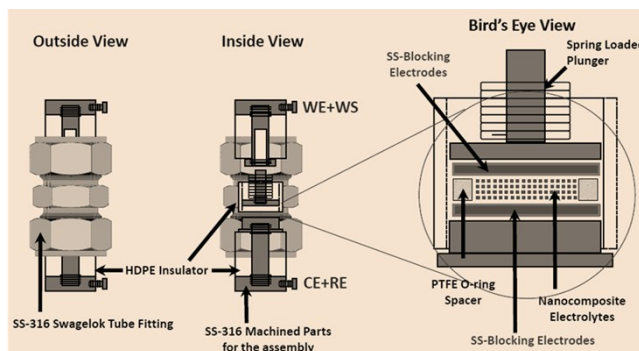


Figure SI-2(a). Typical line diagram illustrating the swagelok-cell assembly in 2-electrode geometry used as sample holders for electrochemical studies.



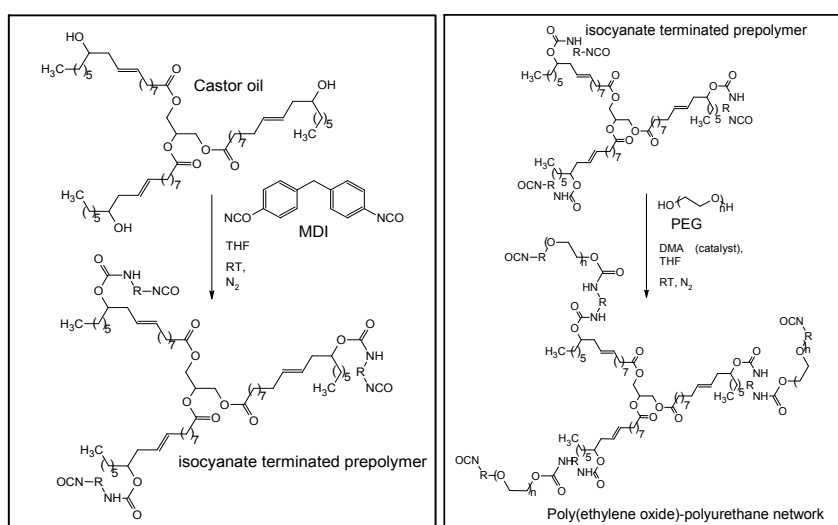
Figure SI-2(b). Typical photographs depicting the experimental set-up used for electrochemical evaluation during an ongoing investigation. The system is interfaced with a thermostated oven equipped with parallel test channels independently connected to spring loaded Swagelok cells to test the samples at identical conditions.

The electrochemical stability window of the electrolyte matrix was determined using linear sweep voltammetry in a Swagelok three-electrode T-assembly, where a 316 stainless steel disk was used as the working electrode while lithium metal served as the counter electrode and reference. The spring load in the Swagelok assembly was ensured to apply similar pressure using Teflon spacer of appropriate dimensions. An anodic scan was carried out on the samples between 2.5 and 7 V at a scan rate of $10 \text{ mV}\cdot\text{s}^{-1}$ and room temperature ($30 \text{ }^\circ\text{C}$) using a Zahner Zennium electrochemical workstation. The direct current (*dc*-) polarization tests were carried out on the same set-up here samples were sandwiched between two 316 stainless steel blocking electrodes along with a Teflon spacer of appropriate dimension and loaded in the leak-proof Swagelok assembly at room temperature. The decay of current in response to a constant applied voltage (1V) was measured as a function of time (6 h). All the synthesized samples were vacuum-dried overnight at $80 \text{ }^\circ\text{C}$ before carrying out the characterizations.

The transference numbers were measured using a technique that combines both the *dc*- and *ac*- polarization methods, first described by Evans *et al.* (Ref: Evans, J.; Vincent, C. A.; Bruce, P. G. *Polymer* **1987**, *28*, 2324.) The electrochemical cell comprised a circular piece of polymer electrolyte sandwiched between two circular non-blocking electrodes made of lithium foil ($\sim 0.98 \text{ cm}^2$). The impedance of the cell was measured between the frequencies of 0.1 Hz and 100 kHz, before and after applying a constant potential difference across the electrodes. Direct current polarization was carried out by applying a constant potential, ranging between 10 mV and 1 V, to the symmetrical cell and resulting current was measured as a function of time. All the measurements were conducted under argon-atmosphere at room temperature.

Synthesis of PEG-PU polymer networks

The poly(ethylene glycol)-polyurethane (PEG-PU) polymer networks were synthesized as described elsewhere and is now well established.^{32,33,47-50} For a typical reaction the total $\text{-NCO/}-\text{OH}$ ratio was maintained at 1.25. Initially, castor oil, CO (-OH value ~ 2.7) and required amount of MDI solution in THF were taken in a round bottomed flask, degassed and stirred for an hour at room temperature under nitrogen atmosphere. To this pre-polymer, a solution of the macromonomer (PEG) in THF along with DMA as catalyst is added and the stirring is continued further for half an hour before casting on a teflon petri-dish. The mix is allowed to dry at room temperature for 24 h followed by oven curing at $80 \text{ }^\circ\text{C}$ for another 48h to obtain a free-standing film of polyethylene glycol-polyurethane (PEG-PU) networks. The schematic pathway of the pre-polymer formation followed by the complete network generated is provided as **Scheme-1** and **Scheme-2**. Aliquots drawn at different time intervals from the reaction mix and different stages of curing are characterized using FTIR to follow the progress of reaction and completion.(provided as **Figure SI-3**).



Scheme-1: Reaction of castor oil and diphenylmethane-4-4'-diisocyanate to give an isocyanate-terminated prepolymer network in the first step of the reaction. **Scheme-2:** Reaction of isocyanate-terminated prepolymer with poly(ethylene glycol) to form poly(ethylene glycol)-polyurethane networks

Castor oil (-OH value ~ 2.7) is one of the essential component. It is primarily comprised of ricinoleic acid chains ($> 90\%$) which, possess tri-hydroxyl functionality and act as the crosslinker for the PEG-PU network formation as described. The urethanation reaction proceeds via simple isocyanate chemistry to almost 97 % conversion (confirmed by soxhlet extraction) with formation of a very stable network. When this network is formed in juxtaposition of another oligomer/polymer (either linear/branched) as in this case with either PEGDME or P(SPM-Li⁺) they can be termed as Semi-IPNs (Ref: Sperling, L. H. In *Interpenetrating Polymer Networks*; Klemperer, D., Sperling, L. H., Utracki, L. A., Eds.; *Advances in Chemistry Series*, ACS: Washington, DC, 1994, Vol. 239).

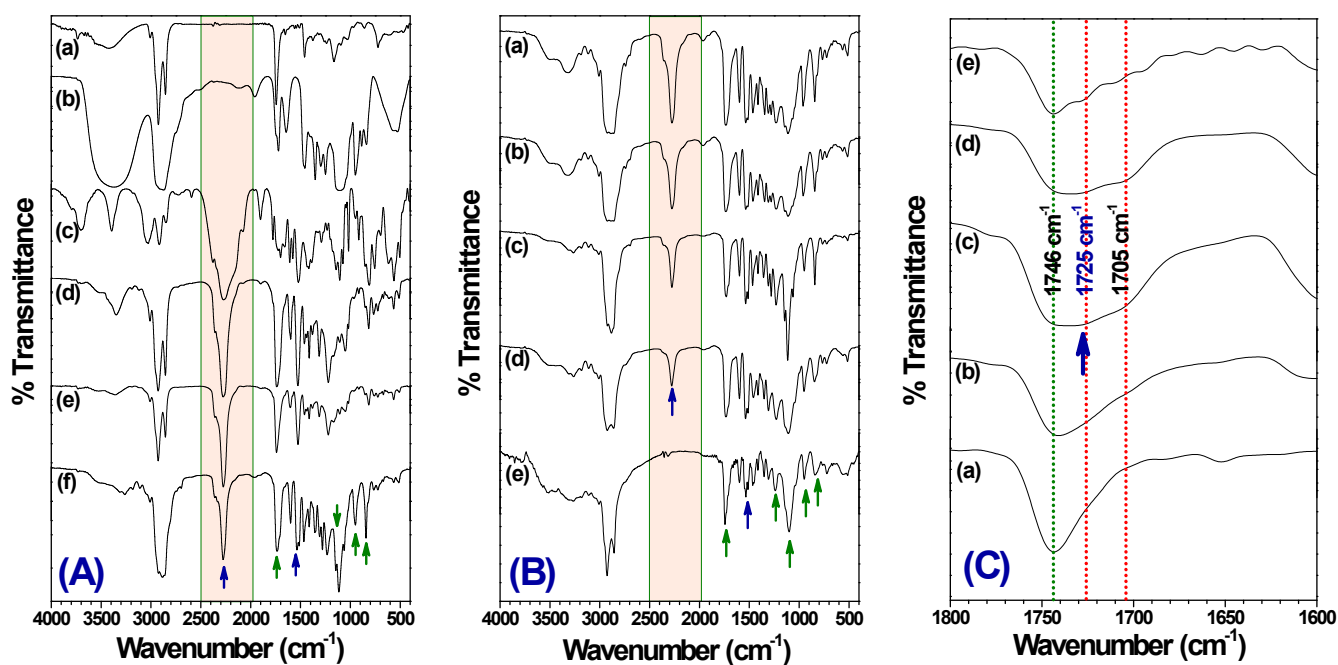


Figure SI-3: Representative FTIR stack plots for the monomers/macromonomers used for the formation of the polyethylene glycol-polyurethane (PEG-PU) network formation. The stack plots (A) and (B) showcases the urethanation reaction at different stages with progressive formation of the network in the reactant mix and finally completion of the reaction post-curing at 80 °C that can be followed as a function of time. The gradual disappearance of the characteristic isocyanate peak at ca. 2270 cm^{-1} is clearly evidenced and the product obtained is a free-standing polyurethane film. (A) FTIR of the pure chemicals used: (a) castor oil (CO); (b) polyethylene glycol, $M_w = 4000$ (PEG); (c) N,N'-diphenylmethane diisocyanate (MDI); Prepolymer formation stage (d) CO+MDI at 0 mins (e) CO+MDI after 60 mins; Initiation of the network formation in presence of dimethylaniline (DMA), a room temperature catalyst (f) post addition of PEG at 0 mins. (B) FTIR plots as a function of time post addition of PEG in the reaction mixture: (a) 15 mins (b) 30 mins (c) 60 mins (d) 180 mins and (e) after 48 hrs of curing at 80 °C. (C) Magnified Wavenumber-scale to highlight the progressive formation of urethane bond ($\sim 1724 \text{ cm}^{-1}$) during reaction: (a) castor oil (CO); (b) CO+MDI after 60 mins; (c) CO+MDI+PEG after 15 mins; (d) CO+MDI+PEG after 60 mins; (e) after 48 hours curing.

The pure castor oil spectrum does show a carbonyl peak at 1746 cm^{-1} (Refer **Figure SI-3(C)**). During the reaction, an initial broadening and then gradual appearance of a peak at $\sim 1725 \text{ cm}^{-1}$ almost merged as a shoulder to the 1746 cm^{-1} peak is indicative of urethane carbonyl. Thus, the shoulder at 1746 cm^{-1} pertaining to the C=O stretching of the urethane linkage indicates the formation of polyethylene glycol-polyurethane networks. The cumulative contribution of the urethane linkage along with the existing castor oil carbonyl peak shows a shift to 1742 cm^{-1} . Concurrently, the signature -NCO peak seen at $\sim 2275 \text{ cm}^{-1}$, disappears completely after 48hrs curing as evident for

the parent network PEG-PU indicating completion of reaction. The strong band corresponding to the C-O-C stretching vibrations at $\sim 1110\text{ cm}^{-1}$ suggests incorporation of the PEG in the network.

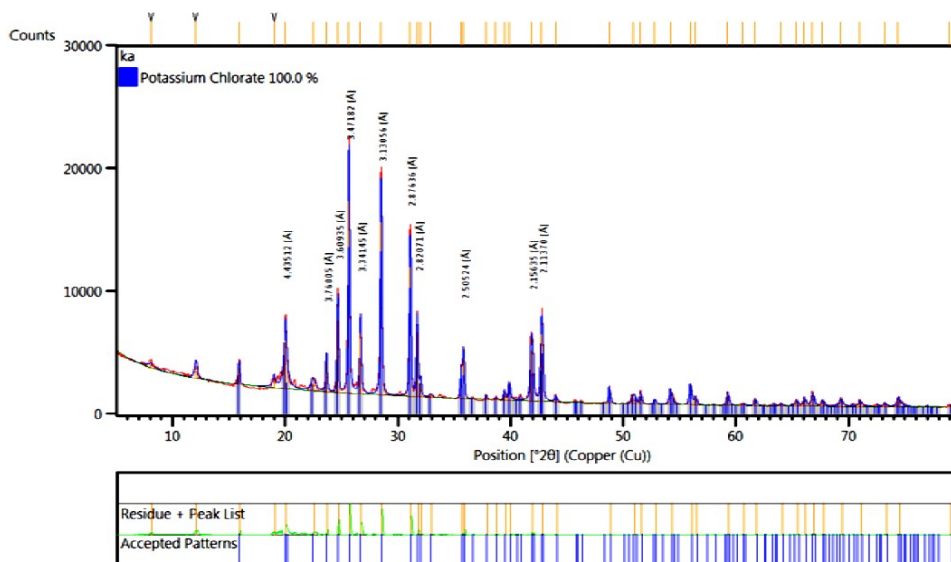


Figure SI-4. X-ray diffraction pattern of the precipitate recovered post ion exchange (lithiation) using LiClO_4 in a THF : AN (50/50 v/v) mixed solvent system. The analysis confirms formation of potassium perchlorate (KClO_4) which is insoluble in the solvent system used and signifies a complete ion-exchange was successfully achieved for the anionic monomer, 3-sulfopropyl methacrylate salt.

Inductively Coupled Plasma–Optical Emission Spectroscopy (ICP-OES) Studies:

Quantitative Estimation of Cation Exchange

The extent of ion exchange was further quantified with ICP-OES analysis employing a Varian 725-ES ICP Optical Emission Spectrometer. The analysis were done in triplicate for separately prepared samples ($N = 3$) with three repetitions for each sample.

Molecular weight of the lithiated anionic monomer = 214

Theoretically, 214 ppm of monomer should yield 7 ppm of Lithium present in the system.

Experimental observations for the supplied sample along with three standard samples were made at two characteristic Lithium wavelengths (460.29 nm and 670.78 nm) as shown in the representative photograph. The readings were average out for the runs.

| Tube | Sample Labels | Li 460.289 ppm | Li 670.783 ppm |
|------|---------------|-------------------|-------------------|
| 1 | Blank | 0.00000 | 0.00000 |
| 2 | Standard 1 | 1.0000 | 1.0000 |
| 3 | Standard 2 | 5.0000 | 5.0000 |
| 4 | Standard 3 | 10.000 | 10.000 |
| 5 | LSPM-1 | 0.55038 | 0.37578 |
| 6 | 1PPM | 0.99762 | 1.0137 |
| 7 | LSPM REPEAT | 0.52250 | 0.36084 |
| 8 | 5PPM | 5.1896 | 5.0904 |
| 9 | LSPMREPEAT | 0.54423 | 0.37285 |
| 10 | Sample 6 | 0.07244u | 0.02031 |
| 11 | Sample 7 | | |
| 12 | Sample 8 | | |

In this typical case for 12.5 ppm of the monomer sample provided:

Averaging $(0.55038+0.37578+0.52250+0.36084+0.54423+0.37285)/6$

$= 2.72658/6 = 0.45443$

$\approx 0.45\text{ ppm of Lithium}$ was observed.

The results signify a 100 % ion exchange taking place.

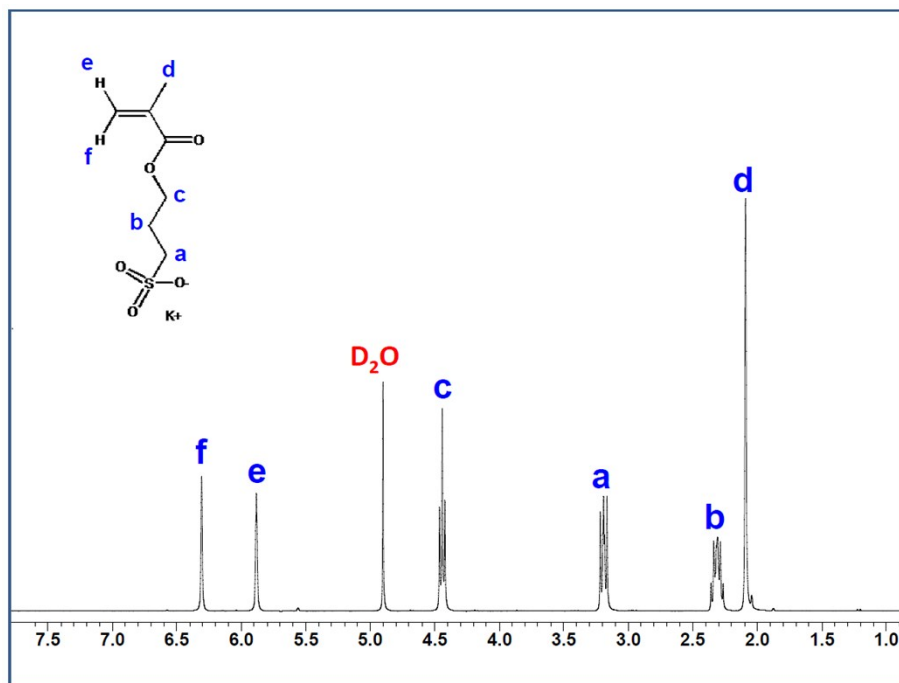


Figure SI-5(a). ¹H-NMR obtained in D₂O for the as procured anionic monomer, 3-sulfopropyl methacrylate potassium salt prior to carrying out the ion-exchange step.

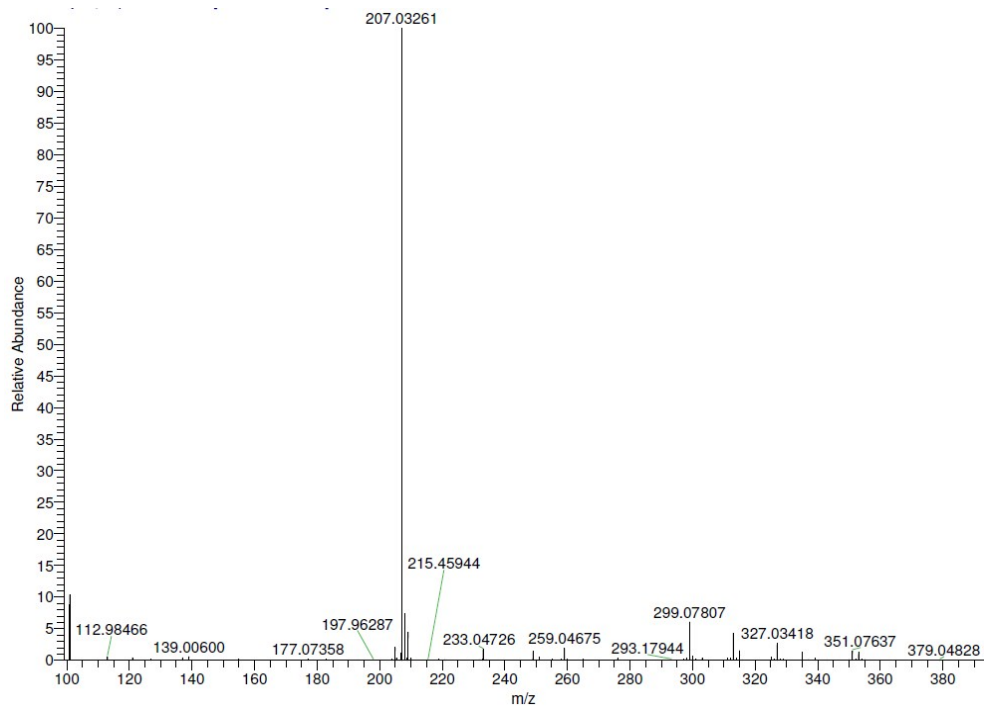


Figure SI-5(b). ESI-MS for the as procured anionic monomer, 3-sulfopropyl methacrylate potassium salt prior to carrying out the ion-exchange step.

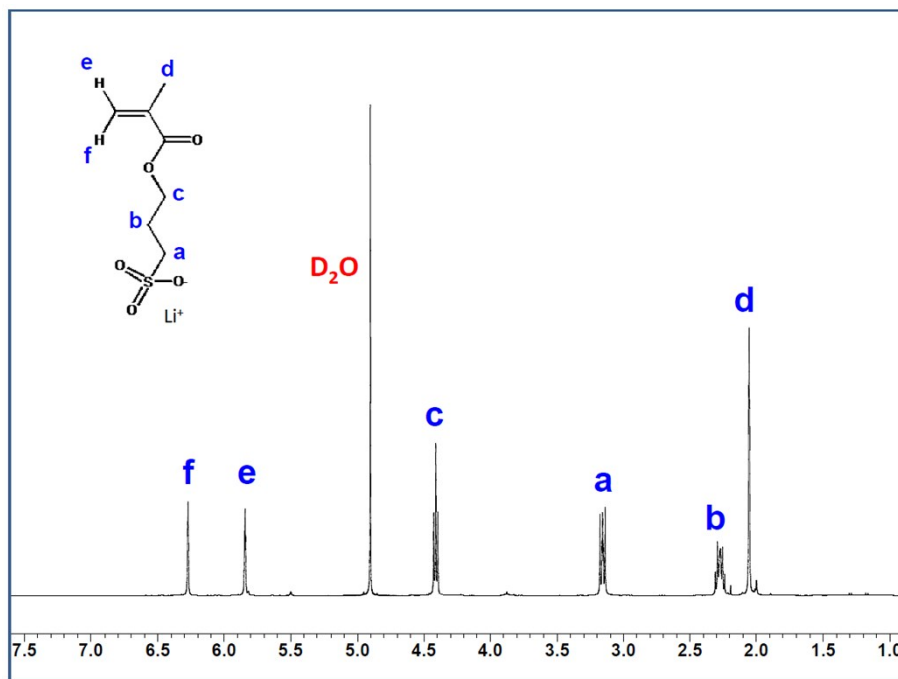


Figure SI-6(a). ¹H-NMR obtained in D₂O for the anionic monomer, 3-sulfopropyl methacrylate lithium salt post ion exchange (lithiation) using LiClO₄ in a THF : AN (50/50 v/v) mixed solvent system.

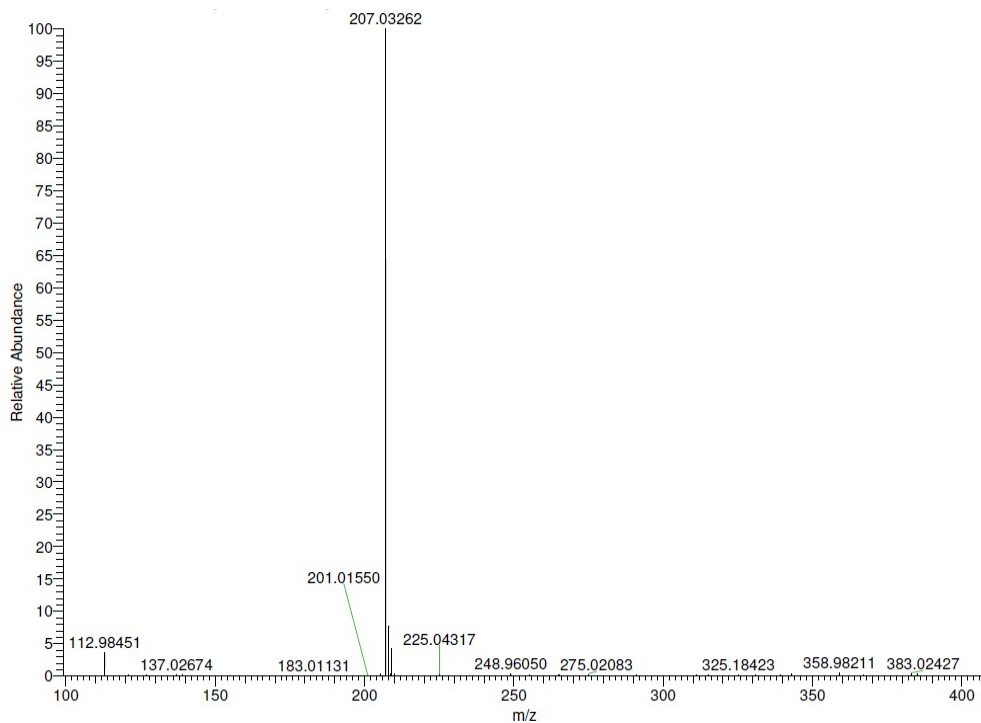


Figure SI-6(b). ESI-MS for the anionic monomer, 3-sulfopropyl methacrylate lithium salt post ion exchange (lithiation) using LiClO₄ in a THF : AN (50/50 v/v) mixed solvent system.

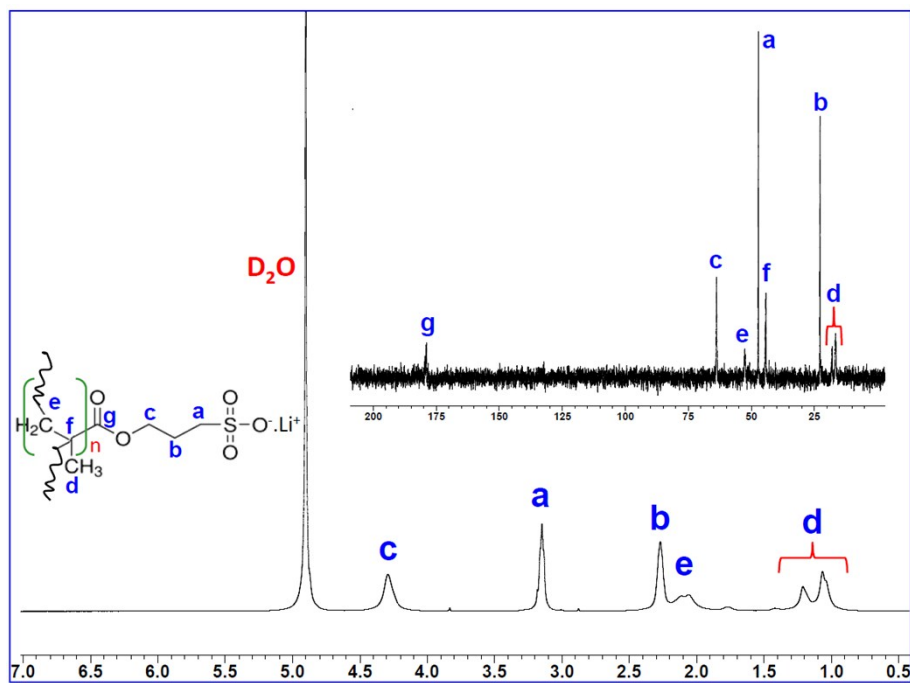


Figure SI-7(a). ^1H -NMR and ^{13}C -NMR (Inset) obtained in D_2O offers structural confirmation for the formation of the anionic polymer chains containing the 3-sulfopropyl methacrylate lithium salt subunits.

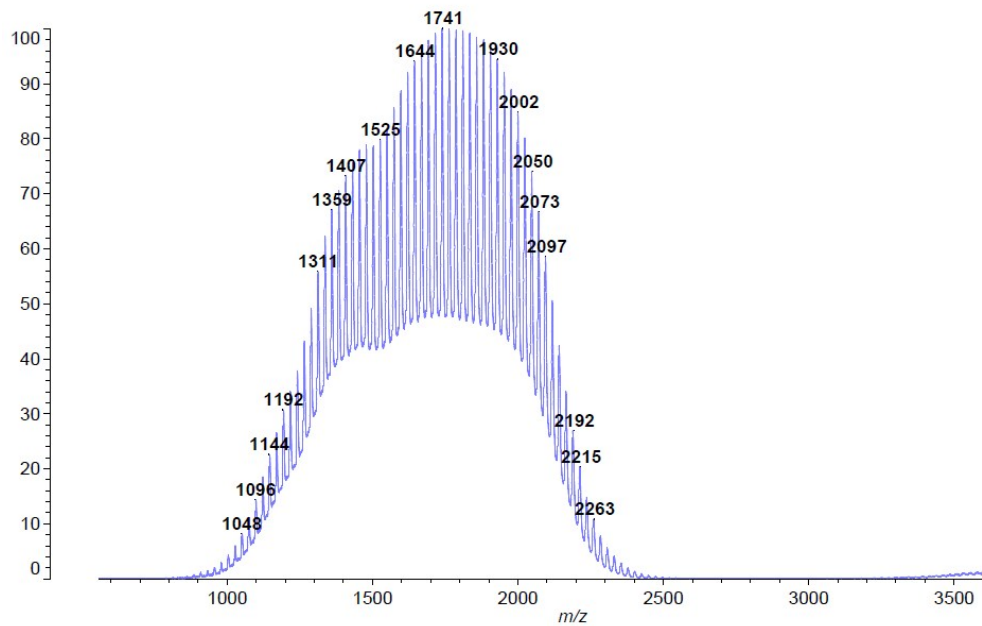


Figure SI-7(b). MALDI-TOF offers confirmation on the molecular weight of the anionic polymer chains containing the 3-sulfopropyl methacrylate lithium salt subunits. The average molecular weight of the oligomers achieved is ~ 1800 Daltons with an degree of polymerization 9 ± 4 units.

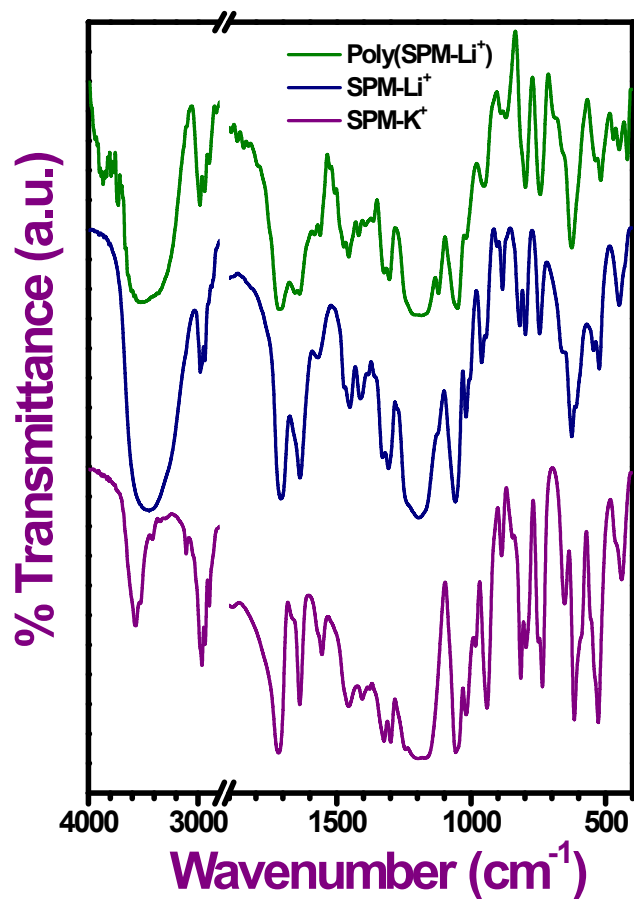


Figure SI-8. Representative mid-FTIR scans for: (a) as procured anionic monomer, 3-sulfopropyl methacrylate potassium salt (b) the anionic monomer used for synthesis, 3-sulfopropyl methacrylate lithium salt post ion exchange (lithiation) and (c) the anionic homopolymer synthesized, P(SPM:Li⁺). The clearly distinguishable peaks in FT-IR spectra from SPM:K⁺ to SPM:Li⁺ is 1057- 1063 cm⁻¹ peak corresponds to the ion exchange of K⁺ to Li⁺, while rest of the peaks does not show much peak shift.

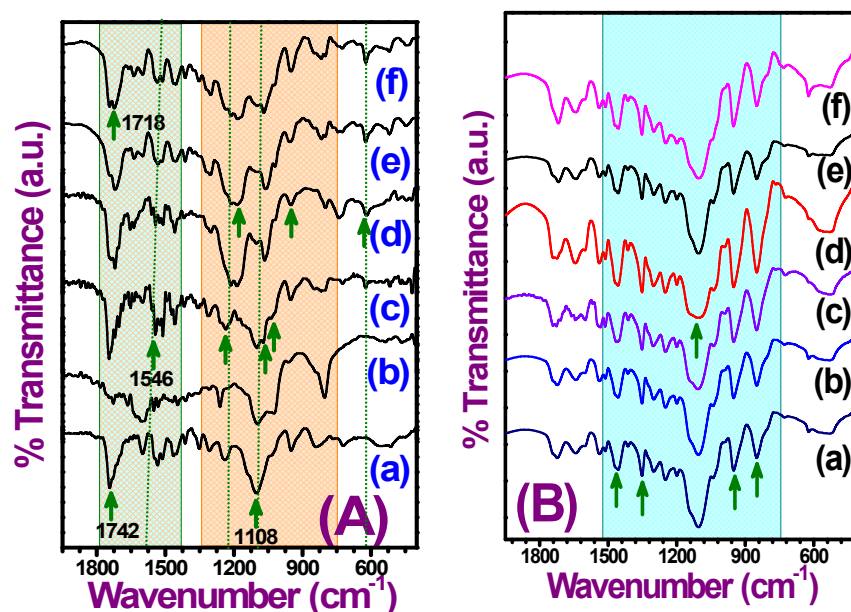


Figure SI-9. Representative mid-FTIR stacked scans of **(A)** binary semi-IPN compositions: **(a)** PEG-PU networks; **(b)** PEG-PU:P(SPM⁻.Li⁺) 80:20; **(c)** PEG-PU: P(SPM⁻.Li⁺) 70:30; **(d)** PEG-PU: P(SPM⁻.Li⁺) 60:40; **(e)** PEG-PU:P(SPM⁻.Li⁺) 50:50; and **(f)** PEG-PU:P(SPM⁻.Li⁺) (40:60); **(B)** ternary semi-IPN compositions of PEG-PU:PEGDME and P(SPM⁻.Li⁺). The amount of P(SPM⁻.Li⁺) incorporated in the compositions is represented as the number of ethylene oxide units available per Li⁺-ion: **(a)** 60:40, EO/Li-25; **(b)** 40:60, EO/Li-25; **(c)** 30:70, EO/Li-50; **(d)** 30:70, EO/Li-30; **(e)** 30:70, EO/Li-20 and **(f)** 30:70, EO/Li-10.

The *polymer-polymer* and *ion-polymer* interactions were quite evident from the mid-FTIR studies (**Figure SI-9(A) and (B)**). The distinctive vibrational bands corresponding to the C-O-C stretching vibration at $\sim 1108 \text{ cm}^{-1}$ along with the broad peak 1746 cm^{-1} from the ester carbonyl of castor oil and polyurethane contribution (1725 cm^{-1} , merged) are highlighted in the scan **Figure 9(A):(a)** for reference.^{33,34} The cumulative contribution of the urethane linkage along with the existing castor oil carbonyl peak shows a shift to 1742 cm^{-1} . With progressive increase in the secondary component, P(SPM⁻.Li⁺) for binary semi-IPN compositions significant changes in the zones of interests are observed. The peak at 1335 cm^{-1} can be attributed to the S=O stretching.⁵³ The doublet at *ca.* 1262 cm^{-1} and 1246 cm^{-1} are ascribed to the asymmetric stretching vibration of the SO₃ group ($\nu_{as}\text{SO}_3$) while the peak at $\sim 1167 \text{ cm}^{-1}$ is the contribution of the symmetric stretch ($\nu_s\text{SO}_3$).^{18,53-55} The noticeable shoulders at *ca.* 1050 cm^{-1} can be assigned the symmetric stretching of the sulfonate groups bound to Li⁺-cation ($-\text{SO}_3^-\cdot\text{Li}^+$) coupled with the stretching modes of free anions ($-\text{SO}_3^-$) at $\sim 1018 \text{ cm}^{-1}$.¹⁸ The peak at *ca.* 730 cm^{-1} can be assigned to the $\nu(\text{C-S})$ along with asymmetric in-plane bending modes of sulfonate is seen at *ca.* 615 cm^{-1} .^{33,34} These apart the interaction of lithium cations with the ester groups are observed at around 1540 cm^{-1} ,¹⁷ partially overlapped alongside N-H bending at *ca.* 1510 cm^{-1} ,³³ while complexation with C-O-C of the networks is particularly evinced from the peak at *ca.* 650 cm^{-1} .⁵⁶ That the interactions occurring between polyether chain segments in the network and the anionic homopolymer incorporated (*polymer-polymer*) are appreciable is indicated by the significantly suppressed peaks at *ca.* 946 cm^{-1} and 844 cm^{-1} (**Figure SI-9A:(b)-(f)**), two characteristic peaks attributed to $r(\text{CH}_2)_5$ observed in polyethers.

Earlier reports have suggested presence of these supports the preferential gauche confirmation of the -CH₂-CH₂- units necessary to attain helical conformation of the PEO chains.⁵⁷

The effect of PEGDME incorporation as the ternary component in the matrix is perceptible, **Figure SI-9B:(a)-(f)**. Apart from the presence of peaks already identified for the anionic homopolymer in the semi-IPN matrix, the characteristic peaks of polyethers are manifested quite distinctly (shown by arrows). Two clear CH₂ vibrational modes appear at *ca.* 1460 cm⁻¹ and \sim 1351 cm⁻¹, which corresponds to asymmetric CH₂ bending, $\delta(\text{CH}_2)_a$ and symmetric CH₂ wagging coupled with C-C stretching ($w(\text{CH}_2)_s + v(\text{CC})$), respectively.^{57,58} The strong reappearance of peaks at *ca.* 946 cm⁻¹ and 844 cm⁻¹ also asserts the formation of helical conformations implying preferential domains of PEG-PU/PEGDME coexisting in the matrix. Additionally, the prominently broad C-O-C regions suggest very favourable ionic interactions and improved ion dissociation that provides crucial clues in understanding the ion-transport behaviour in these ternary matrices discussed in the following sections.

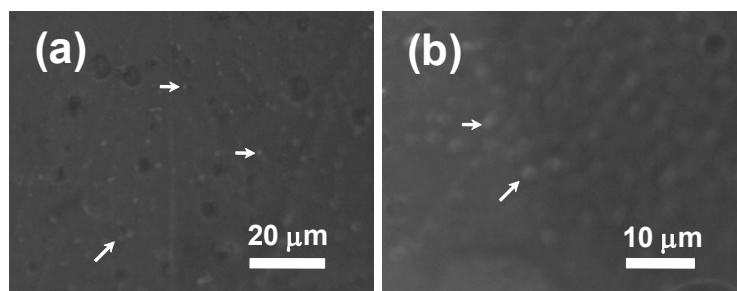


Figure SI-10. Representative micrographs **(a)** optical images of PEG-PU/P(SPM·Li⁺) blends. Arrows indicates the phase separated domains of the P(SPM·Li⁺) when blended with the PEG-PU matrix *ex-situ* **(b)** magnified image.

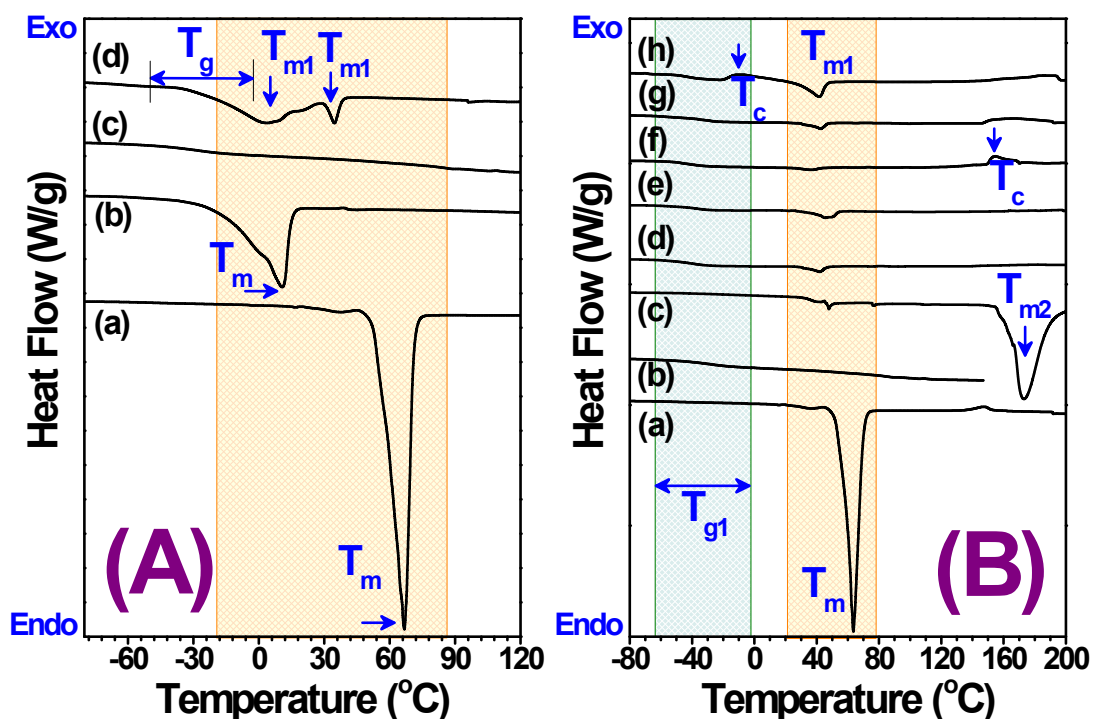


Figure SI-11. (A) Representative DSC stack plots of macromonomer used, oligomer, polymer networks and semi-IPN (a) pure polyethylene glycol (PEG), $M_w = 4000$, (b) polyethylene glycol dimethylether (PEGDME) $M_w = 500$, (c) polyethylene glycol-polyurethane networks (PEG-PU) (d) semi-IPN PEG-PU/PEGDME, $M_w = 500$. (B) Stack plots of (a) PEG macromer used, $M_w \sim 4000$ (repeated for reference); (b) polyurethane networks PEG-PU; (c) homopolymer, P(SPM.Li⁺), $M_w \sim 1800$; the synthesized semi-IPNs of variable compositions: (d) PEG-PU:P(SPM.Li⁺), 80:20; (e) PEG-PU:P(SPM.Li⁺), 70:30; (f) PEG-PU:P(SPM.Li⁺), 60:40; (g) PEG-PU:P(SPM.Li⁺), 50:50 and (h) PEG-PU:P(SPM.Li⁺), 40:60. A broad glass transition temperature for all semi-IPN compositions were observed well below room temperature. Evidently a slight increase in crystalline contribution with addition of P(SPM.Li⁺) component signifies induced ordering in the PEG domains.

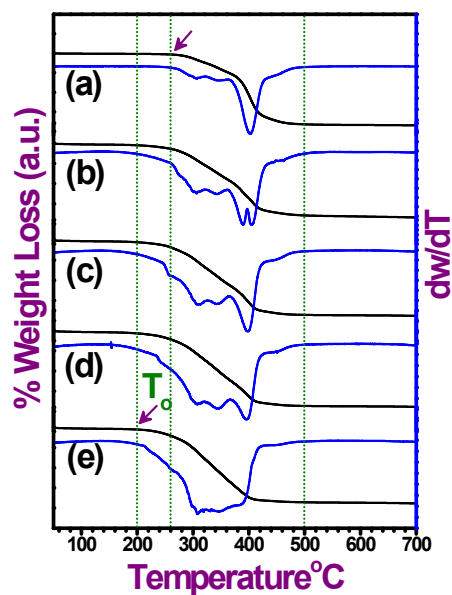


Figure SI-12. Representative TG-DTA double-axis stack plots of the synthesized semi-IPN matrices with increased amounts of PEGDME (a) PEG-PU; (b) PEG-PU:PEGDME (70:30); (c) PEG-PU:PEGDME (50:50); (d) PEG-PU:PEGDME (40:60); and (e) PEG-PU:PEGDME (30:70). All the compositions maintained a P(SPM:Li⁺) concentration such that the EO/Li⁺ mole ratio = 25.

Thermal stability of these synthesized ternary semi-IPNs were evaluated using thermogravimetry (**Figure SI-12** and **Table 1**). The parent network incorporating P(SPM:Li⁺) displayed a thermal degradation onset of ~250 °C along with the three degradation stages conventionally observed for most polyurethane networks.³³ The first stage corresponds to scission of ether/ester linkages, the second stage corresponds to the degradation of the urethane linkages and the third advanced fragmentation and charring. With increase in the content of polyethylene glycol dimethylether (tertiary component), the degradation profiles noticeably shifted towards lower temperatures with obvious merging of the first and second degradation stages at high loading of the PEGDME (30:70). The appearance of multiple steps in the differential plots for interim compositions indicates the apparent inter-/intra- molecular interactions of the polymeric/oligomeric chains and degradation of those domains. Overall, the ternary semi-IPNs were found to be appreciably stable up to ~160 °C implying their suitability for device applications.

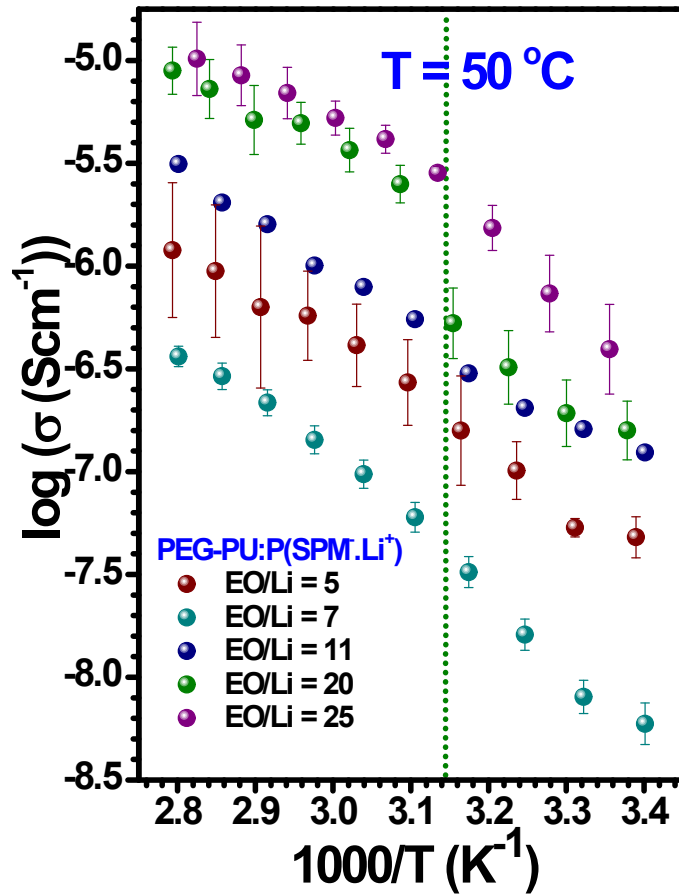


Figure SI-13. Typical Arrhenius plots of ionic conductivity for different weight ratio of P(SPM·Li⁺) incorporated into the PEG-PU network (binary compositions). The EO/Li mole ratio indicates the amount of P(SPM·Li⁺) with respect to the number of EO units of the polyethylene glycol in the network.

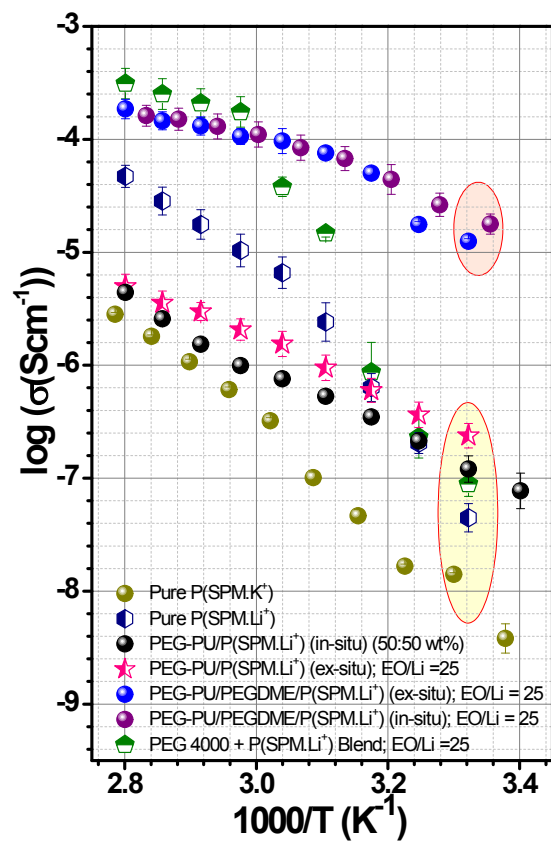


Figure SI-14. Representative plots depicting ionic conductivity ($\text{Log}\sigma$) behavior as a function of temperature for pure single-ion conducting homopolymer (K^+ , Li^+ salt), solution blends of binary compositions and ternary compositions. The EO/Li mole ratio indicates the amount of P(SPM.Li⁺) with respect to the number of EO units of the available in the matrix (*i.e.* PEG used in the network + PEGDME). The weight ratio of PEG-PU:PEGDME used in the compositions is 50:50. The notation *ex-situ* and *in-situ* for P(SPM.Li⁺) refers to how the anionic homopolymer has been incorporated in the system. *Ex-situ* implies formation of the films using solution blending while *in-situ* refers to the semi-IPN formation where the incorporation of P(SPM.Li⁺) in the growing network is achieved using mutually exclusive reaction strategy.

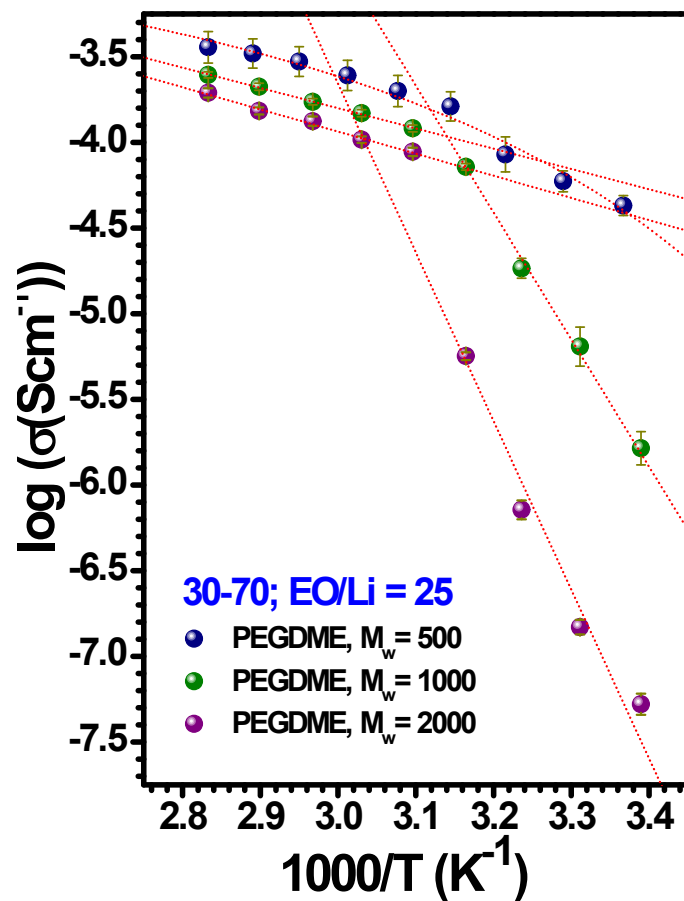


Figure SI-15. Representative plots depicting ionic conductivity ($\text{Log}\sigma$) behavior as a function of temperature for ternary compositions with variations in PEGDME molecular weights. The EO/Li mole ratio indicates the amount of P(SPM⁺:Li⁺) with respect to the number of EO units of the available in the matrix (*i.e.* PEG used in the network + PEGDME). The weight ratio of PEG-PU:PEGDME used in the compositions is 30:70.

Mechanism of Ionic Conduction:

Key research findings by many notable groups over the years have established the Li⁺-ion solvation and transport within the –C-O-C– cage (Ref: Ratner, M. A.; Shriver, D. F. Ion Transport in Solvent-Free Polymers. *Chem. Rev.* **1988**, 88, 109–124; Gray, F. M. *Polymer Electrolytes*; The Royal Society of Chemistry: Cambridge, UK, **1997**; *Macromolecules* **2012**, 45, 6230–6240; *Macromolecules* **2008**, 41, 5723–5728; *Macromolecules* **2011**, 44, 5381–5391; *Phys. Rev. E* **2013**, 88, 052602). The mechanism of ionic conduction in polymeric electrolytes particularly comprising of PEG/PEO based materials is a well studied system. The ion solvation particularly the cations (Li⁺) in these systems are aided by formation of transient crosslinks with the ether oxygen. Most researchers agree that the number of crosslinks that solvates the cation (Li⁺) involves at least four oxygen atom at any given time, which resembles a –C-O-C– cage (refer to the schematic provided below). It is also understood that optimal conductivity is usually seen at salt concentrations ranges with approximately 10-25 ethylene oxide (EO) unit per lithium cation. Apart from the ionic hopping that can take place between the occupied and vacant sites as understood by the reviewer, the ionic conductivity is also assisted by the random segmental motions (internal Brownian motions) that play a key role in these macromolecular matrices. The schematic provided shows a representation of this random walk model (owing to conformational changes in polymeric chain segments above glass transition temperatures) that leads to cleavage and reformation of the transient crosslinks in three dimensional matrices. Effectively a translational change in the Li⁺-ion coordinating site and the polyether chains is observed. Thus polymeric architecture allowing faster segmental motions contributes to higher ionic mobility and charge transport. This phenomenon is also reflected in the Arrhenius plots as a deviation from linearity and has been explained by the empirical Vogel-Tamman-Fulcher (VTF) equation; $\sigma = \sigma_0 \cdot T^{-0.5} \exp\{-E_a/k(T-T_0)\}$.

